Procedia Manufacturing

Volume 5, 2016, Pages 362–374

44th Proceedings of the North American Manufacturing Research Institution of SME http://www.sme.org/namrc

Experimental Validation of Period-n Bifurcations in Milling

Andrew Honeycutt and Tony L. Schmitz
University of North Carolina at Charlotte, Charlotte, NC
ahoney15@uncc.edu, tony.schmitz@uncc.edu

Abstract
This paper describes numerical and experimental analyses of milling bifurcations, or instabilities. The time-delay equations of motions that describe milling behavior are solved numerically for low radial immersion conditions and Poincaré maps are used to study the stability behavior, including secondary Hopf and period-n bifurcations. The numerical studies are complemented by experiments where milling vibration amplitudes are measured under both stable and unstable conditions. The vibration signals are sampled once per tooth period to construct experimental Poincaré maps. The results are compared to numerical stability predictions. The sensitivity of milling bifurcations to changes in natural frequency is also predicted and observed.

Keywords: Machine tool, milling, dynamics, stability, bifurcation

1 Introduction

Decades of machining simulation and measurement research has led to significant understanding of milling process dynamics. In 1946 Arnold reported on chatter in steel machining (Arnold). Doi and Kato described self-excited vibrations using time-delay differential equations in 1956 (Doi and Kato). During this time, the notion of "regeneration of waviness" was promoted as the feedback mechanism (time-delay term), where the previously cut surface combined with the instantaneous vibration state dictates the current chip thickness, force level, and corresponding vibration response (Tobias and Fishwick, Tlusty and Polacek, Tobias, Merritt). This work resulted in analytical algorithms that were used to produce the now well-known stability lobe diagram that separates the spindle speed-chip width domain into regions of stable and unstable behavior (Tobias, Merritt, Tlusty and Polacek, Shridar et al. 1968a, Hohn et al., Shridar et al. 1968b, Hanna and Tobias, Tlusty and Ismail 1981, Tlusty and Ismail 1983, Tlusty 1985, Tlusty 1986, Minis and Yanusevsky, Altintas and Budak).

More recently, Davies et al. used once per revolution sampling to characterize the synchronicity of cutting tool motions (measured using a pair of orthogonal capacitance probes) with the tool rotation in milling (Davies et al. 1998). This approach was an experimental modification of the Poincaré maps used to study state space orbits in nonlinear dynamics. They observed the traditional quasi-periodic

 Selection and peer-review under responsibility of the Scientific Programme Committee of NAMRI/SME

doi:10.1016/j.promfg.2016.08.031

chatter associated with the secondary (subcritical) Hopf, or Neimark-Sacker, bifurcation that can occur for systems described by periodic time-delay differential equations (Moon and Kalmár-Nagy).

In 2000, Davies *et al.* further examined the stability of highly interrupted (or low radial immersion) milling (Davies *et al*. 2000). They reported a doubling of the number of optimally stable spindle speeds when the time in cut is small (i.e., low radial depth of cut). In 2001, Moon and Kalmár-Nagy reviewed the "prediction of complex, unsteady and chaotic dynamics" in machining (Moon and Kalmár-Nagy). They listed the various contributors to nonlinear behavior, including the loss of tool-workpiece contact due to large amplitude vibration and workpiece material constitutive relations, and highlighted previous applications of nonlinear dynamics methods to the study of chatter (Moon, Bukkapatnam *et al.*, Stépán and Kalmár-Nagy, Nayfey *et al.*, Minis and Berger, Moon and Johnson). They also specified the use of phase-space methods, such as Poincaré maps, to identify changes in machining process dynamics.

Time-domain simulation offers a powerful tool for exploring milling behavior and has been applied to identify instability (Smith and Tlusty, Campomanes and Altintas). For example, Zhao and Balachandran implemented a time-domain simulation which incorporated loss of tool-workpiece contact and regeneration to study milling (Zhao and Balachandran). They identified secondary Hopf bifurcation and suggested that "period-doubling bifurcations are believed to occur" for low radial immersions (Zhao and Balachandran). They included bifurcation diagrams for limited axial depth of cut ranges at two spindle speeds to demonstrate the two bifurcation types.

Davies *et al.* extended their initial work in 2002 to present the first analytical stability boundary for highly interrupted machining (Davies *et al*. 2002). It was based on modeling the cutting process as a kicked harmonic oscillator with a time delay and followed the two-stage map concept described previously (Davies *et al*. 2000). They used the frequency content of a microphone signal to establish the existence of both secondary Hopf and period-2 (period-doubling or flip) instabilities. Mann *et al*. also provided experimental validation of secondary Hopf and period-2 instabilities for up and down milling (Mann *et al*. 2003b). They reported "a kind of period triple phenomenon" (Mann *et al*. 2003b) observed using the once-per-revolution sampled displacement signal recorded from a single degree of freedom flexure-based machining platform.

The semi-discretization, time finite element analysis, and multi-frequency methods were also developed to produce milling stability charts that demonstrate both instabilities (Mann *et al*. 2003, Insperger *et al*. 2003, Insperger and Stépán, Mann *et al*. 2004, Merdol and Altintas Y). In (Govekar *et al*.), it was shown using the semi-discretization method that the period-2 bifurcation exhibits closed, lens-like, curves within the secondary Hopf lobes, except for the highest speed stability lobe. The same group (Gradišek *et al*.) reported further experimental evidence of quasi-periodic (secondary Hopf), period-2, period-3, period-4, and combined quasi-periodic and period-2 chatter, depending on the spindle speed-axial depth values for a two degree of freedom dynamic system. A perturbation analysis was performed in (Mann *et al*. 2005) to identify the secondary Hopf and period-2 instabilities. Additionally, numerical integration was implemented to construct a bifurcation diagram for a selected spindle speed that demonstrated the transition from stable operation to quasi-periodic chatter as the axial depth is increased.

Stépán *et al*. continued to explore the nonlinear aspects of milling behavior in 2005 (Stépán *et al*.). They described stable period-2 motion where the tool does not contact the workpiece in each tooth period (even in the absence of runout). For a two flute cutter, for example, only one tooth contacts the workpiece per revolution; they referred to this condition as the "fly over effect" and included a bifurcation diagram for these proposed stable and unstable period-2 oscillations.

The effect of the helix angle on period-2 instability was first studied by (Zatarain *et al.*). They found that, depending on the helix angle, the closed, lens-like, curves within the secondary Hopf lobes change their size and shape. They also found that these closed islands of stability can appear even in the highest speed stability lobe (in contrast to the results when helix angle is not considered). Experimental results were provided. This work was continued in (Insperger *et al*. 2006), where the

authors emphasized that, at axial depths equal to the axial pitch of the cutter teeth, the equation of motion becomes an autonomous delay differential equation so the period-2 instability is not possible. Patel *et al*. also studied the helix effect in up and down milling using the time finite element approach (Patel *et al*.).

In this paper, period-n bifurcations are experimentally identified for n = 2, 3, 6, 7, and 15. Additionally, the sensitivity of the bifurcation behavior to system dynamics is explored. A comparison of numerical simulation predictions and experiments is also presented.

2 Poincaré Maps

In this study, Poincaré maps were developed using both experiments and simulations. For the experiments, the displacement and velocity of the flexible workpiece were recorded and then sampled once per tooth period. In simulation, the displacement and velocity were predicted, but the same sampling strategy was applied. By plotting the displacement versus velocity, the phase space trajectory can be observed in both cases. The once per tooth period samples are then superimposed and used to interrogate the milling process behavior. For stable cuts, the motion is periodic with the tooth period, so the sampled points repeat and a single grouping of points is observed. When secondary Hopf instability occurs, the motion is quasi-periodic with tool rotation because the chatter frequency is (generally) incommensurate with the tooth passing frequency. In this case, the once per tooth sampled points do not repeat and they form an elliptical distribution. For period-2 instability, on the other hand, the motion repeats only once every other cycle (i.e., it is a sub-harmonic of the forcing frequency). In this case, the once per tooth sampled points alternate between two solutions. For period-n instability, the sampled points appear at n locations.

3 Time-domain Simulation

Time-domain simulation entails the numerical solution of the governing equations of motion for milling in small time steps. It is well-suited to incorporating all the intricacies of milling dynamics, including the nonlinearity that occurs if the tooth leaves the cut due to large amplitude vibrations and complicated tool geometries (including runout, or different radii, of the cutter teeth, non-proportional teeth spacing, and variable helix). The simulation is based on the Regenerative Force, Dynamic Deflection Model described by (Smith and Tlusty). As opposed to stability lobe diagrams that provide a "global" picture of the stability behavior, time-domain simulation provides information regarding the "local" cutting force and vibration behavior (at the expense of computational efficiency) for the selected cutting conditions. The simulation used in this study proceeds as follows:

1. the instantaneous chip thickness is determined using the vibration of the current and previous teeth at the selected tooth angle
2. the cutting force is calculated
3. the force is used to find the new displacements
4. the tooth angle is incremented and the process is repeated. Modal parameters are used to describe the system dynamics in the x (feed) and y directions, where multiple degrees of freedom in each direction can be accommodated.

The instantaneous chip thickness depends on the nominal, tooth angle-dependent chip thickness, the current vibration in the direction normal to the surface, and the vibration of previous teeth at the same angle. The chip thickness can be expressed using the circular tool path approximation as $h(t) = f_t \sin(\phi) + n(t-\tau) - n(t)$, where f_t is the commanded feed per tooth, ϕ is the tooth angle, n

is the normal direction, and τ is the tooth period. The tooth period is defined as $\tau = \frac{60}{\Omega N_t}$ (sec), where Ω is the spindle speed in rpm and N_t is the number of teeth. The vibration in the direction of the surface normal for the current tooth depends on the x and y vibrations as well as the tooth angle according to $n = x\sin(\phi) - y\cos(\phi)$.

For the simulation, the strategy is to divide the angle of the cut into a discrete number of steps. At each small time step, dt, the cutter angle is incremented by the corresponding small angle, $d\phi$. This approach enables convenient computation of the chip thickness for each simulation step because: 1) the possible teeth orientations are predefined; and 2) the surface created by the previous teeth at each angle may be stored. The cutter rotation $d\phi = \frac{360}{SR}$ (deg) depends on the selection of the number of steps per revolution, SR. The corresponding time step is $dt = \frac{60}{SR \cdot \Omega}$ (sec). A vector of angles is defined to represent the potential orientations of the teeth as the cutter is rotated through one revolution of the circular tool path, $\phi = [0, d\phi, 2\,d\phi, 3\,d\phi, \ldots, (SR-1)\,d\phi]$. The locations of the teeth within the cut are then defined by referencing entries in this vector.

In order to accommodate the helix angle for the tool's cutting edges, the tool may be sectioned into a number of axial slices. Each slice is treated as an individual straight tooth endmill, where the thickness of each slice is a small fraction, db, of the axial depth of cut, b. Each slice incorporates a distance delay $r\chi = db\tan(\gamma)$ relative to the prior slice (nearer the cutter free end), which becomes the angular delay between slices: $\chi = \frac{db\tan(\gamma)}{r} = \frac{2db\tan(\gamma)}{d}$ (rad) for the rotating endmill, where d is the endmill diameter and γ is the helix angle. In order to ensure that the angles for each axial slice match the predefined tooth angles, the delay angle between slices is $\chi = d\phi$. This places a constraint on the db value. By substituting $d\phi$ for χ and rearranging, the required slice width is $db = \frac{d \cdot d\phi}{2\tan(\gamma)}$.

Using the time-domain simulation approach, the forces and displacements may be calculated. These results are then sampled once-per-tooth period to generate the bifurcation diagrams.

4 Experimental Results

A single degree of freedom (SDOF) flexure was used to define the system dynamics. Modal impact testing verified that the cutting tool dynamic stiffness (1055 Hz natural frequency, 0.045 viscous damping ratio, and 4.2×10^7 N/m stiffness) was much higher than the SDOF flexure. The flexure setup also simplified the measurement instrumentation. The flexure motions were measured using both a laser vibrometer and a low mass accelerometer. In order to enable once per tooth sampling of the vibration signals, a laser tachometer was used. A small section of reflective tape was attached to the tool and the corresponding laser tachometer signal used to perform the once per tooth sampling.

The cutting tool was a 20 mm diameter, single flute carbide square endmill. Modal impact testing verified that the cutting tool stiffness was much higher than the SDOF flexure. Each cut of the 6061-T6 aluminum workpiece was performed using a feed per tooth of 0.10 mm/tooth.

Cutting tests were completed using the Fig. 1 setup. The measured flexure dynamics and cutting conditions are listed in Table 1. Results for period-2, 3, 6, 7, and 15 bifurcations are displayed in Figs. 2-7. In each figure, the left plot shows the simulated behavior and the right plot shows the experimental result. Good agreement is observed in each case.

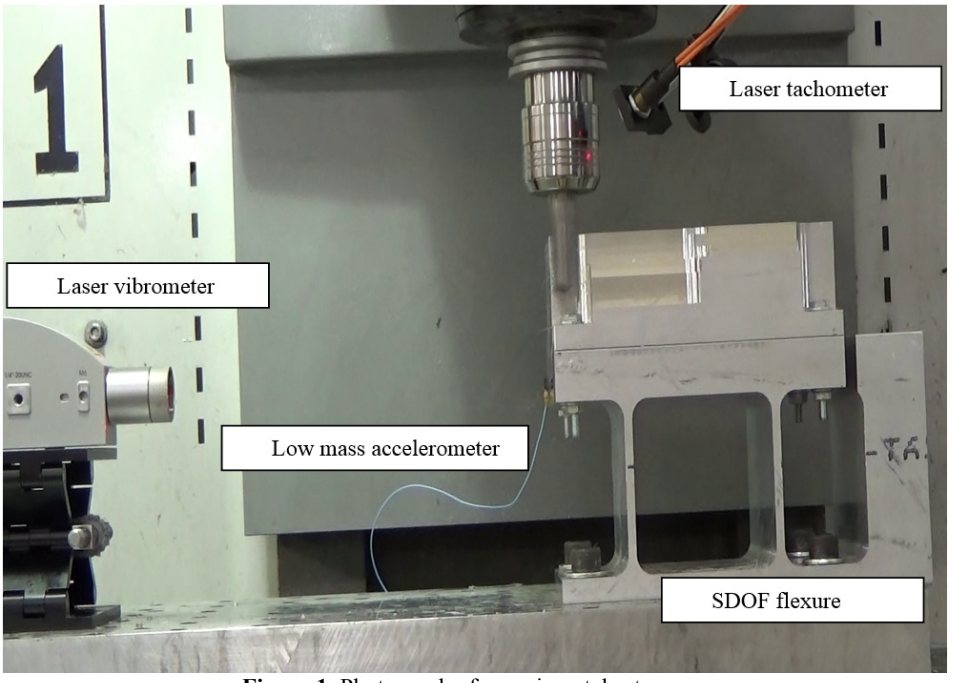

Figure 1. Photograph of experimental setup.

Table 1. Cutting conditions and flexure dynamics for experiments.

	Cutting conditions			**Flexure dynamics**		
Period-n	Spindle speed (rpm)	Axial depth, b (mm)	Radial depth (mm)	Stiffness (N/m)	Natural frequency (Hz)	Damping ratio (%)
2	3486	2.0	1	9.0×10^5	83.0	2.00
3	3800	4.5	5	5.6×10^6	163.0	1.08
6	3200	18.0	1	5.6×10^6	202.6	0.28
6	3250	15.5	1	5.6×10^6	205.8	0.28
7	3200	14.5	1	5.6×10^6	204.1	0.28
15	3200	14.0	1	5.6×10^6	204.8	0.28

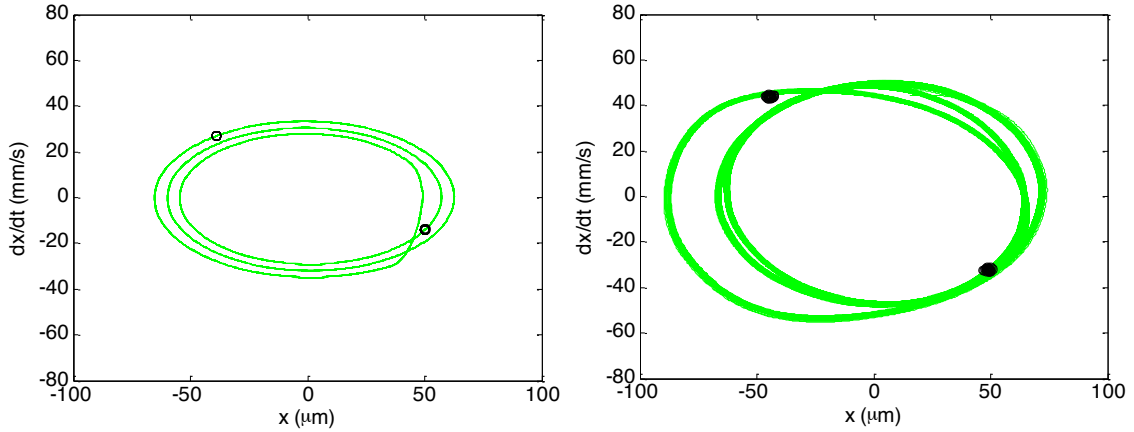

Figure 2. Poincaré section for period-2 bifurcation. (Left) simulation, (right) experiment.

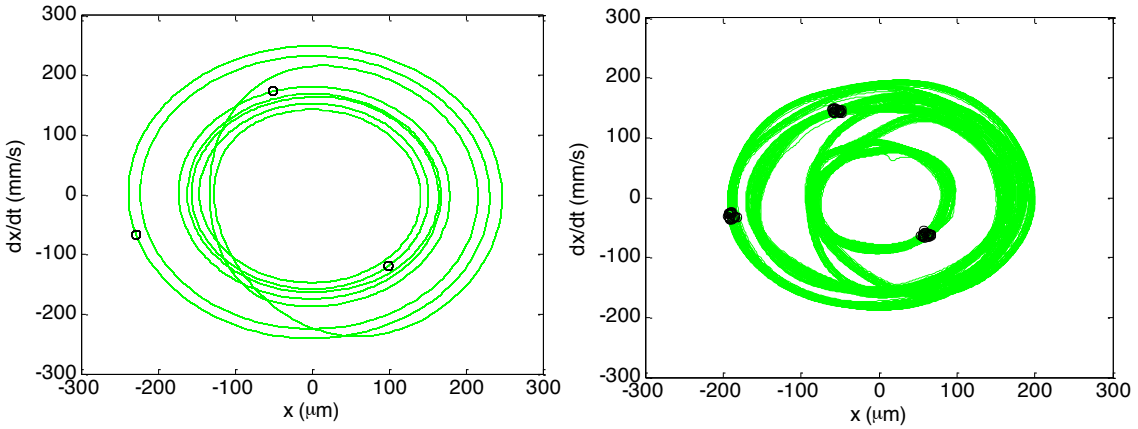

Figure 3. Poincaré section for period-3 bifurcation. (Left) simulation, (right) experiment.

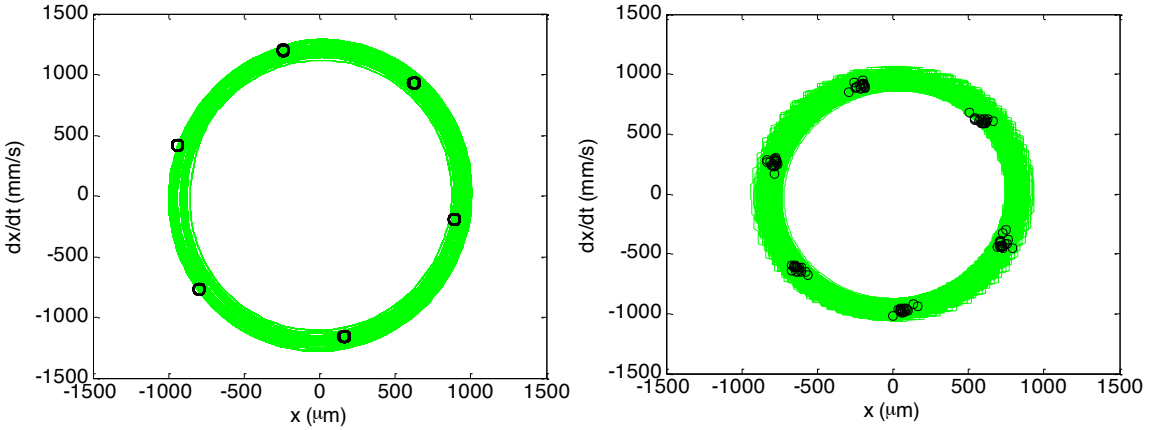

Figure 4. Poincaré section for period-6 bifurcation. (Left) simulation, (right) experiment.

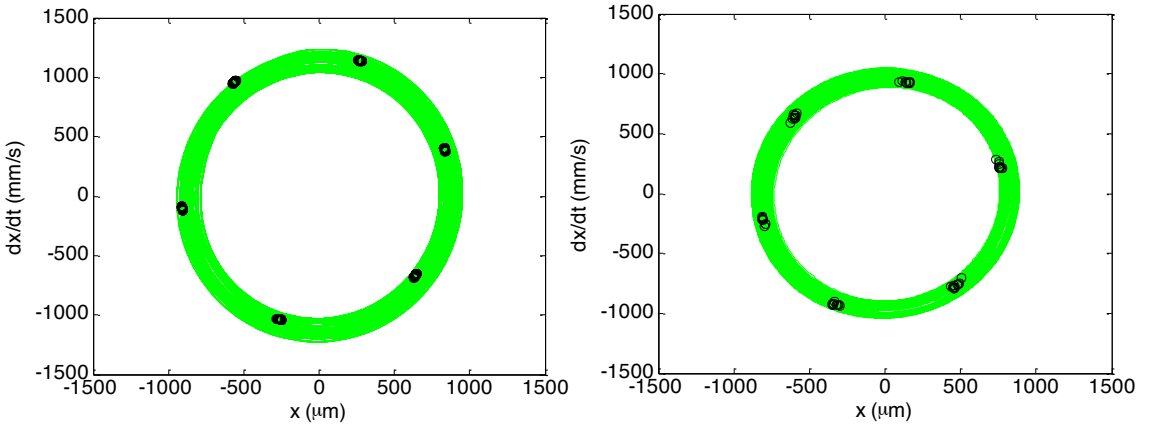

Figure 5. Poincaré section for a second period-6 bifurcation. (Left) simulation, (right) experiment.

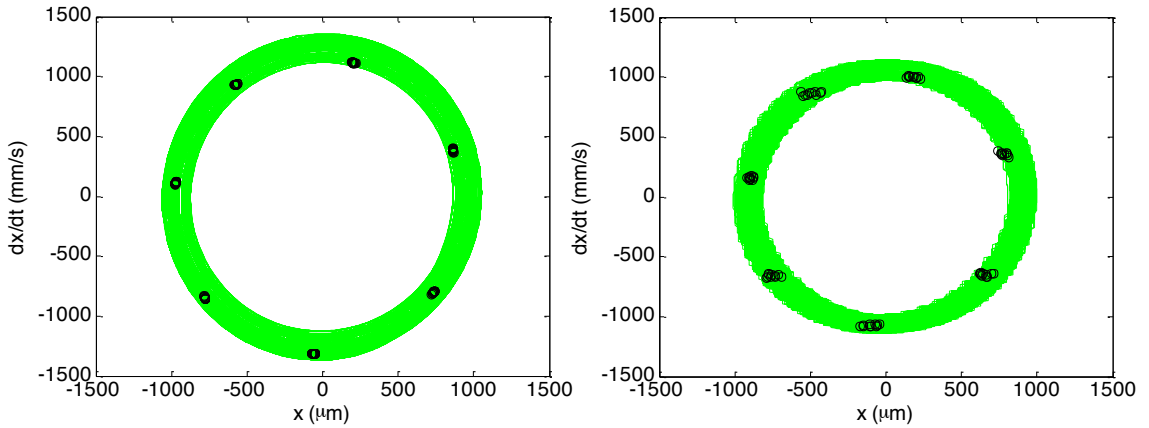

Figure 6. Poincaré section for period-7 bifurcation. (Left) simulation, (right) experiment.

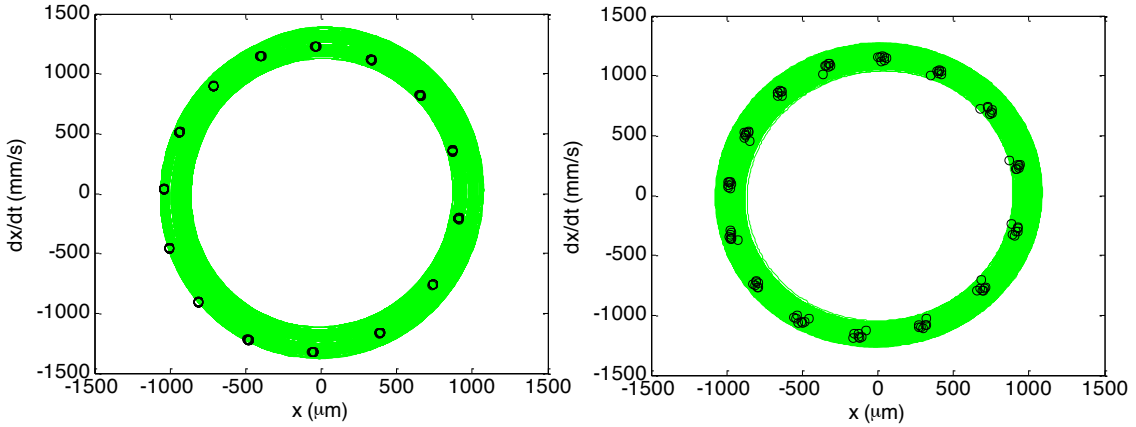

Figure 7. Poincaré section for period-15 bifurcation. (Left) simulation, (bottom) experiment.

Experiments were also completed to demonstrate the sensitivity of the period-n bifurcation behavior to changes in natural frequency. During cutting, material is removed from the workpiece which lowers the workpiece mass and, subsequently, increases the flexure's natural frequency. Since the mass of the chips is much smaller than the workpiece, these changes result in small changes in natural frequency. The changes in system dynamics for the experiments presented in Figs. 9-12 are provided in Table 2. The higher period-n bifurcations exhibited sufficient sensitivity to flexure natural frequency that, within a single cut, both period-n bifurcation and quasi-periodic behavior were observed.

Table 2. Changes in flexure natural frequency due to mass removal.

	Flexure dynamics				**Cutting conditions**		
Period-n (figure number)	Natural frequency at the beginning of the cut (Hz)	Natural frequency at the end of the cut (Hz)	Change in natural frequency (Hz)	Change in mass (g)	Spindle speed (rpm)	Axial depth, b (mm)	Radial depth (mm)
6 (8)	202.4	202.7	0.3	4.8	3200	18.0	1
6 (9)	205.7	205.9	0.2	4.1	3250	15.5	1
7 (10)	204.1	204.3	0.2	3.9	3200	14.5	1
15 (11)	204.7	204.9	0.2	3.7	3200	14.0	1

Figures 8-11 show the flexure's feed (x) direction velocity (dx/dt) versus time. The continuous signal is displayed as a solid line, while the circles are the once-per-tooth sampled points. In each figure, the left plot shows the simulated behavior and the right plot shows the experimental behavior. Good agreement is observed. The time-domain simulation was altered to account for the changing natural frequency due to mass loss. After each time step, the change in mass was calculated based on the volume of the removed chip and the density of the workpiece material. This change in mass was then used to update the flexure's natural frequency for the next time step.

A summary of the behavior seen in Figs. 8-11 is provided here.

1. Figure 8 exhibits period-6 behavior from 4 to 11 s, followed by quasi-periodic behavior until the end of the cut.

2. Figure 9 shows period-6 behavior from 4 to 13 s and then quasi-periodic behavior is observed until the end of the cut.
3. Figure 10 displays quasi-periodic behavior from the beginning of the cut until 11 s and then period-7 behavior from 11 to 15 s.
4. Figure 11 exhibits quasi-periodic behavior from the beginning of the cut until 8 s, period-15 behavior from 8 to 13 s, and then quasi-periodic behavior until the end of the cut

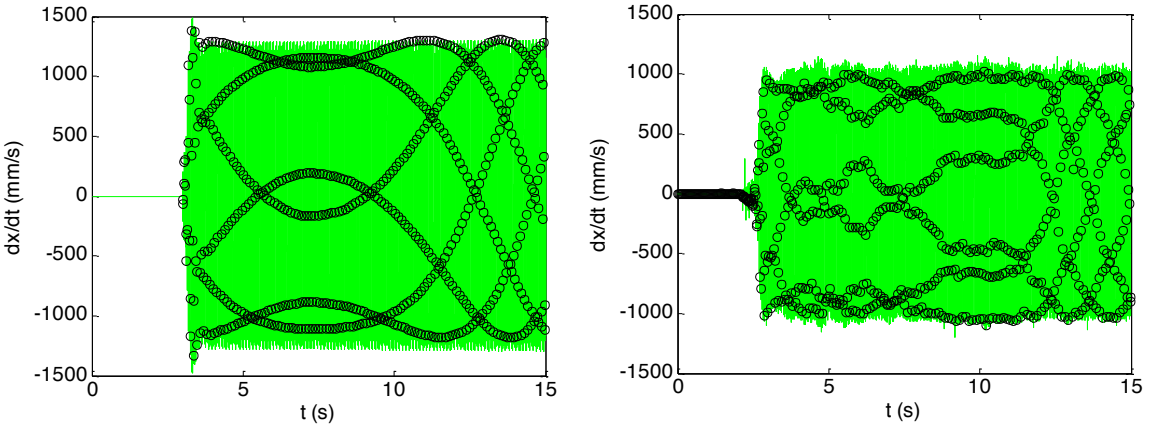

Figure 8. Variation in bifurcation behavior with changes in natural frequency. Period-6 bifurcation is observed. (Left) simulation, (right) experiment.

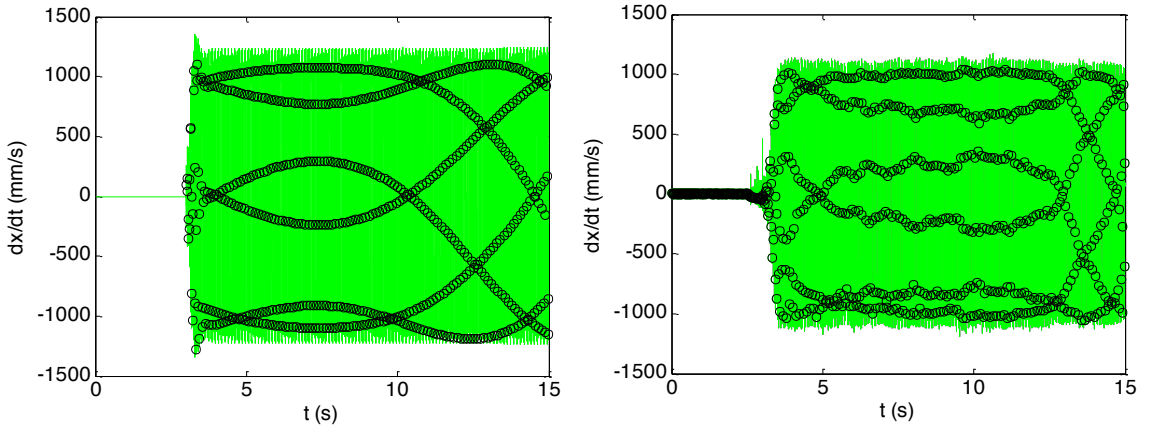

Figure 9. Variation in bifurcation behavior with changes in natural frequency. Period-6 bifurcation is observed. (Left) simulation, (right) experiment.

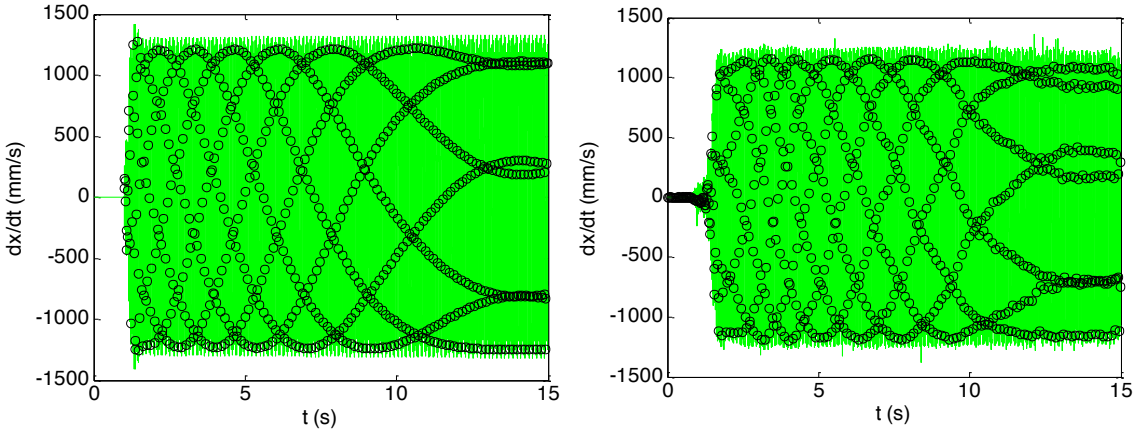

Figure 10. Variation in bifurcation behavior with changes in natural frequency. Period-7 bifurcation is observed. (Left) simulation, (right) experiment.

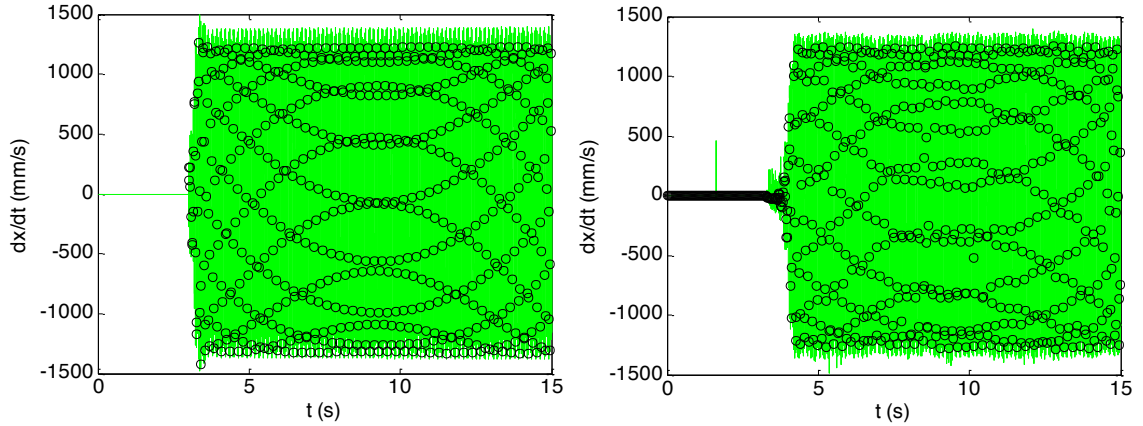

Figure 11. Variation in bifurcation behavior with changes in natural frequency. Period-15 bifurcation is observed. (Left) simulation, (right) experiment.

5 Conclusions

This paper described numerical and experimental analyses of milling bifurcations. Numerical simulation was used to solve the time-delay equations of motions that describe milling behavior and Poincaré maps were used to study the stability behavior, including secondary Hopf and period-n bifurcations. Experiments were completed where milling vibration amplitudes were measured under both stable and unstable conditions. The vibration signals were sampled once per tooth period to construct experimental Poincaré maps. The results were compared to numerical stability predictions. The sensitivity of milling bifurcations to changes in natural frequency was also predicted and observed.

6 Acknowledgements

This material is based upon work supported by the National Science Foundation under Grant No. CMMI-1561221.

References

Altintas Y and Budak E. Analytical prediction of stability lobes in milling. *Annals of the CIRP* 1995; 44(1): 357-362.

Arnold RN. The mechanism of tool vibration in the cutting of steel, In: *Proceedings of the Institute of Mechanical Engineers*, 1946, p. 154.

Bukkapatnam S, Lakhtakia A, and Kumara S. Analysis of senor signals shows turning on a lathe exhibits low-dimensional chaos. *Physics Review E* 1995; 52: 2375-2387.

Campomanes ML and Altintas Y. An improved time domain simulation for dynamic milling at small radial immersions. *ASME Journal of Manufacturing Science and Engineering* 2003; 125(3): 416-422.

Davies MA, Dutterer BS, Pratt JR, and Schaut AJ. On the dynamics of high-speed milling with long, slender endmills. *Annals of the CIRP* 1998; 47(1): 55-60.

Davies MA, Pratt JR, Dutterer BS, and Burns TJ. The stability of low radial immersion milling. *Annals of the CIRP* 2000; 49(1): 37-40.

Davies MA, Pratt JR, Dutterer BS, and Burns TJ. Stability prediction for low radial immersion milling, *ASME Journal of Manufacturing Science and Engineering* 2002; 124: 217-225.

Doi S and Kato S. Chatter vibration of lathe tools. *Transactions of the ASME* 1956; 78: 1127-1134.

Govekar E, Gradišek J, Kalveram M, Insperger T, Weinert K, Stépán G, and Grabec I. On stability and dynamics of milling at small radial immersion. *Annals of the CIRP* 2005; 54(1): 357-362.

Gradišek J, Kalveram M, Insperger T, Weinert K, Stépán G, Govekar E, and Grabec I. On stability prediction for milling. *International Journal of Machine Tools and Manufacture* 2005; 45(7-8): 769-781.

Hanna NH and Tobias SA. A theory of nonlinear regenerative chatter. *ASME Journal of Engineering of Industry* 1974; 96: 247-255.

Hohn RE, Shridar R, and Long GW. A stability algorithm for a special case of the milling process, *ASME Journal of Engineering for Industry* 1968; 90: 326-329.

Insperger T, Muñoa J, Zatarain MA, and Peigné G. Unstable islands in the stability chart of milling processes due to the helix angle, In: *CIRP 2nd International Conference on High Performance Cutting*, Vancouver, Canada, 2006.

Insperger T and Stépán G. Vibration frequencies in high-speed milling processes or A positive answer to Davies, Pratt, Dutterer, and Burns. *ASME Journal of Manufacturing Science and Engineering* 2004; 126(3): 481-487.

Insperger T, Stépán G, Bayly PV, and Mann BP. Multiple chatter frequencies in milling processes. *Journal of Sound and Vibration* 2003; 262: 333-345.

Mann BP, Bayly PV, Davies MA, and Halley JE. Limit cycles, bifurcations, and accuracy of the milling process. *Journal of Sound and Vibration* 2004; 277: 31-48.

Mann BP, Garg NK, Young KA, and Helvey AM. Milling bifurcations from structural asymmetry and nonlinear regeneration. *Nonlinear Dynamics* 2005; 42(4): 319-337.

Mann BP, Insperger T, Bayly PV, and Stépán G. Stability of up-milling and down-milling, Part 1: Alternative analytical methods. *International Journal of Machine Tools and Manufacture* 2003; 43(1): 25-34.

Mann BP, Insperger T, Bayly PV, and Stépán G. Stability of up-milling and down-milling, Part 2: Experimental verification. *International Journal of Machine Tools and Manufacture* 2003; 43(1): 35-40.

Merdol SD and Altintas Y. Multi frequency solution of chatter stability for low immersion milling. *ASME Journal of Manufacturing Science and Engineering* 2004; 126: 459-466.

Merritt HE. Theory of self-excited machine-tool chatter. *ASME Journal of Engineering for Industry* 1965; 87: 447-454.

Minis I and Berger BS. Modelling, analysis, and characterization of machining dynamics, In: *Dynamics and Chaos in Manufacturing Processes* (Ed. F.C. Moon), Wiley, 1998, pp. 125-163.

Minis I and Yanusevsky R. A new theoretical approach for prediction of chatter in milling. *ASME Journal of Engineering for Industry* 1993; 115: 1-8.

Moon FC. Chaotic dynamics and fractals in material removal processes. In: *Nonlinearity and Chaos in Engineering Dynamics* (Ed. J. Thompson and S. Bishop), Wiley, 1994, pp. 25-37.

Moon FC and Johnson M. Nonlinear dynamics and chaos in manufacturing processes, In: *Dynamics and Chaos in Manufacturing Processes* (Ed. F.C. Moon), Wiley, 1998, pp. 3-32.

Moon FC and Kalmár-Nagy T. Nonlinear models for complex dynamics in cutting materials. *Philosophical Transactions of the Royal Society London A* 2001; 359: 695-711.

Nayfey A, Chin C, and Pratt J. Applications of perturbation methods to tool chatter dynamics. In: *Dynamics and Chaos in Manufacturing Processes* (Ed. F.C. Moon), Wiley, 1998, pp. 193-213.

Patel BR, Mann BP, and Young KA. Uncharted islands of chatter instability in milling. *International Journal of Machine Tools and Manufacture* 2008; 48(1): 124-134.

Schmitz T and Smith KS. *Machining Dynamics: Frequency Response to Improved Productivity*. New York: Springer, 2009.

Shridar R, Hohn RE, and Long GW. A general formulation of the milling process equation. *ASME Journal of Engineering for Industry* 1968; 90: 317-324.

Shridar R., Hohn RE, and Long GW. A stability algorithm for the general milling process. *ASME Journal of Engineering for Industry* 1968; 90: 330-334.

Smith KS and Tlusty J. An overview of modeling and simulation of the milling process. *ASME Journal of Engineering for Industry* 1991; 113: 169-175.

Stépán G and Kalmár-Nagy T. Nonlinear regenerative machine tool vibrations. In: *Proceedings of the 1997 ASME Design Engineering Technical conference on Vibration and Noise*. Sacramento, CA, DETC 97/VIB-4021, 1997, pp. 1-11.

Stépán G, Szalai R, Mann BP, Bayly PV, Insperger T, Gradisek J, and Govekar E. Nonlinear dynamics of high-speed milling – Analyses, numerics, and experiments. *Journal of Vibration and Acoustics* 2005; 127: 197-203.

Tobias SA. *Machine Tool Vibration*. New York: Wiley, 1965.

Tobias SA and Fishwick W. The chatter of lathe tools under orthogonal cutting conditions. *Transactions of the ASME* 1958; 80: 1079-1088.

Tlusty J. Machine dynamics, In: *Handbook of High-speed Machining Technology* (Ed. R.I. King). New York: Chapman and Hall, 1985, pp. 48-153.

Tlusty J. Dynamics of high-speed milling, *ASME Journal of Engineering for Industry* 1986; 108: 59-67.

Tlusty J and Ismail F. Basic non-linearity in machining chatter. *Annals of the CIRP* 1981; 30: 299-304.

Tlusty J and Ismail F. Special aspects of chatter in milling. *ASME Journal of Vibration, Stress and Reliability in Design* 1983; 105: 24-32.

Tlusty J and Polacek M. The stability of machine tools against self-excited vibrations in machining. In: *Proceedings of the ASME International Research in Production Engineering Conference*, Pittsburgh, PA, 1963, pp. 465-474.

Tlusty J and Polacek M. Experience with analysing stability of machine tool against chatter. In: *Proceedings of the 9th MTDR Conference*, 1968, pp. 521-570.

Zatarain M, Muñoa J, Peigné G, and Insperger T. Analysis of the influence of mill helix angle on chatter stability. *Annals of the CIRP* 2006; 55(1): 365-368.

Zhao MX and Balachandran B. Dynamics and stability of milling process. *International Journal of Solids and Structures* 2001; 38: 2233-2248.